

ON THE IMPROVEMENT OF LATTICE PERFECTION
IN HIGH PURITY ZINC CRYSTALS GROWN
FROM THE MELT

Thesis for the Degree of M. S.
MICHIGAN STATE UNIVERSITY

Chi Kwun Chyung

1962

This is to certify that the

thesis entitled

ON THE IMPROVEMENT OF LATTICE PERFECTION
IN HIGH PURITY ZINC CRYSTALS GROWN
FROM THE MELT

presented by

Chi Kwun Chyung

has been accepted towards fulfillment
of the requirements for

Master's degree in Metallurgical Engineering

W. E. Gayler, Jr.
Major professor

Date 26 Oct 1962



ON THE IMPROVEMENT OF LATTICE PERFECTION
IN HIGH PURITY ZINC CRYSTALS GROWN
FROM THE MELT

by
Chi Kwun Chyung

A THESIS

Submitted to
Michigan State University
in partial fulfillment of the requirements
for the degree of

MASTER OF SCIENCE

Department of Metallurgy, Mechanics
and Material Science

1962

5-1000

ON THE IMPROVEMENT OF LATTICE PERFECTION
IN HIGH PURITY ZINC CRYSTALS GROWN
FROM THE MELT

by Chi Kwun Chyung

High purity zinc single crystals of controlled orientation have been grown by improving the soft-mold technique. Improvement in crystal perfection was made by (a) minimizing radial thermal stresses during the growth and cooling to room temperature; (b) preventing the propagation of sub-boundaries from the seed.

The best crystals grown were substantially free from sub-boundaries, except a few polygonization sub-boundaries near the free surface. Total dislocation density of such crystals was found to be in the range of $6-9 \times 10^4 \text{ cm}^{-2}$, as revealed by etch figures on sections nearly parallel to the prism plane. The disorientation of the polygonization sub-boundaries ranges from 5 to 30 seconds of arc.

The pseudo Kossel patterns of the crystals produced by the divergent X-ray method showed qualitative agreement with the results obtained by the etching technique on crystal perfection.

Chi Kwun Chyung

The etching technique was capable of measuring much smaller sub-boundary disorientation than the X-ray technique.

ACKNOWLEDGEMENTS

The author wishes to express gratitude to Dr. William E. Taylor for the guidance in this work. The helpful suggestions and encouragements given by Dr. C. T. Wei are also gratefully acknowledged. The entire staff of the Department of Metallurgy, Mechanics and Material Science are thanked for their assistance and helpful discussions. The author wishes to express special gratitude to Mr. and Mrs. Fred R. Fitzpatrick for their spiritual guidance. Finally, he would like to thank the Atomic Energy Commission for the financial helps granted under the Contract #AT (11-1)-1042.

TABLE OF CONTENTS

	Page
INTRODUCTION	1
THEORY AND BACKGROUND	8
EXPERIMENTAL	21
RESULTS AND DISCUSSION	39
CONCLUSIONS	65
RECOMMENDATIONS	67
REFERENCES	70

LIST OF FIGURES

Figure	Page
A. The effective stresses causing plastic flow in the case of radial heat flow	11
1. Furnace set-up (schematic)	33
2. Crucible design	34
3. Crystal growth specimens	34
a) Offset specimen	
b) Standard specimen	
4. Orientations of the crystals and the seeds with their designations	35
5. Furnace set-up	36
6. Furnace control panel	37
7. Acid string saw	38
8. Crystallographic arrangements of sub-boundaries 500x	55
9. Crystallographic arrangements of sub- boundaries. 500x	55
10 & 11. Sub-boundaries propagated from the seed. 500x.	56
12. Background dislocations revealed on:	
a) the cross sectional surface. 500x	57
b) the surface parallel to the growth direction. 500x	57
13. Sub-boundary etching on:	
a) the cross sectional surface. 500x	58
b) the surface parallel to the growth direction. 500x	58

Figure		Page
14.	Effect of crucible size on sub-boundary formation near a corner of the cross sectional surface. 500x	59
	a) crystal grown in the crucible A	
	b) crystal grown in the crucible B	
15.	Sub-boundaries on the cross sectional surface 35x	60
16.	Typical sub-boundaries formed at the faster cooling rate (2 mm/min.) 320x	61
17.	Microfocus x-ray back-reflection pattern of the crystal Y	62
18.	Microfocus x-ray back-reflection pattern of the crystal C	63

I. INTRODUCTION

The existence of imperfections in crystal structure has long been recognized. As early as 1912, Laue found that the intensities of X-ray diffraction spots were not in agreement with the simple theory based on the perfectly arranged crystal lattice. Darwin explained the intensities in terms of "mosaic" structure in which perfect lattice blocks of finite size are slightly disoriented with respect to each other (1). In 1934 Buerger introduced the concept of lineage structure (2). The idea was based on the fact that if inhomogeneous warping occurs between neighboring regions of a crystal during the growth, low angle boundaries are formed at which the crystal orientation changes discontinuously.

Meanwhile in the same year, Taylor (3) and Orowan (4) introduced, independently, the concept of dislocations. This concept was proposed to account for the large discrepancies between the theoretical and experimentally observed strength of crystals. Since then, the theory of dislocations has had a great success in explaining many other properties of crystals.

With gradual development in the experimental techniques of observing dislocations, the theory of dislocations made a

giant stride toward the better understanding of crystalline materials. In the meantime, the growth of crystals free of dislocations became one of the most pursued subjects which might bring still further understanding in the nature of dislocations.

During the past decade, the growth of dislocation--free crystals reached the realm of possibility. Dash has grown dislocation--free silicon crystals (5). The growth of perfect germanium crystals soon followed (6). However, the growth of dislocation--free metallic crystals has not been reported until recently. Elbaum and Howe (9) have grown aluminum crystals free of dislocations in the core. The portions of the crystals free of dislocations were less than about 0.5 mm in diameter. Perfect metallic crystals of substantially large size have not been grown. The growth of perfect metallic crystals would be a difficult task indeed in light of the fact that metals are extremely susceptible to plastic deformation by thermally or mechanically induced stresses during growth as well as during cooling to room temperature.

Much effort in growing perfect crystals from the melt has centered around the elimination of the four most important sources of dislocations (5, 6, 7, 8, 11, 12, 13, 16, 18).

They are: 1) seed, 2) collapsing vacancy disks, 3) thermal stresses, and 4) impurities.

The mechanism of collapsing vacancy disks for the formation of dislocations in crystals grown from the melt has become a center of considerable speculation in recent years. Theoretical calculations made by Schoeck and Tiller (28) show that this mechanism could not account for the formation of "striation" type sub-boundaries. It was noted earlier that Frank's mechanism for striation formation (29) requires that the dislocation loops, once formed behind the interface, must be able to climb towards the moving interface at such a rate that they can catch up with it. The rough calculations made for the climb rate of dislocation loops in metals by Elbaum (8), Schoeck and Tiller (28) differ as much as five orders within the range of typical thermal conditions of careful growth.

The aluminum crystals grown by Howe and Elbaum, free of dislocations in the portions of less than about 0.5 mm in diameter, contained dislocation in the surface layers. The presence of dislocations in the surface layers raises a doubt as to whether the observations can be accounted entirely by the vacancy condensation mechanism.

In the meantime, thermal stress is known to be capable of introducing dislocations in crystals, if such stress is

large enough. Therefore, it is of interest to improve the degree of perfection in metallic crystals grown from the melt by eliminating thermal stresses under proper growth condition.

A similar approach has been initiated by Noggle (15) in his soft-mold technique in which radial heat loss is minimized by soft mold materials of high thermal insulation. The aluminum crystals grown by this technique show comparable degree of perfection to that of crystals grown by strain annealing (20, 21). This is a promising result and should be further improved. In this work, attempts were made to improve the soft-mold technique, thus improve the perfection of metallic crystals grown. Special emphasis was made on eliminating sub-boundaries. If sub-boundaries could be eliminated, it would be a critical test for Schoeck and Tiller's contention in which they argue that Frank's mechanism for lineage formation is inapplicable (28).

The first systematic study on the lineage structures in metal crystals was made by Tetsoonian and Chalmers (16). They have termed the lineage structure as "striations" and were the first ones to propose a mechanism for its formation. Some interesting observations were made on the striations present in tin (99.987 per cent pure) crystals. At slow growth rate the striations tend to form in a direction

parallel to the direction of heat flow, regardless of the crystallographic orientation of the crystal. An incubation distance is necessary before striations can form in those parts of the crystal into which they are not propagated from pre-existing striations. They then explain the formation of the striations in terms of a vacancy condensation mechanism. This implies that the striations do not necessarily propagate from the seed. They also observed that the difference of orientation between neighboring striations is always a rotation of about $1/4$ to 5° about an axis nearly parallel to specimen axis. The density of dislocations contained in striation sub-boundaries was found to be of the order of 10^7 cm^{-2} which was based on the relation $\theta = \frac{b}{h}$, where θ is the angle of disorientation, b is the Burger's vector and h is the spacing between the dislocations in the array. Total dislocation density was of the order of 10^8 cm^{-2} .

Tetsoonian and Chalmers have grown striation-free crystals by reducing temperature gradients. Aust and Chalmers (32) have also grown striation-free crystals by controlling the shape of the solid-liquid interface. The interfaces convex to the liquid and inclined to the specimen axis were used. However, it is doubtful as to whether sub-boundaries

of very small disorientation were absent when the dislocation density is of the order of 10^8 cm^{-2} (32).

Aluminum single crystals grown by the Noggle's soft-mold technique were much more perfect, as examined by X-ray diffraction (20). Here the dislocation density in sub-boundaries was about 10^5 cm^{-2} . The total dislocation density in these crystals was about 10^6 cm^{-2} . Later Kelly and Wei (21) also investigated the perfection of aluminum crystals, grown by Noggle's method, using the fine X-ray beam technique of Schultz. The misorientation of the sub-boundaries in the crystals varied from 1 to 20 minutes of arc. The high perfection of these aluminum crystals was attributed to the low thermal conductivity of the mold. Thus, the reduction in thermal strain during the growth seemed to result in greater perfection. However, no mechanism for the formation of striation type sub-boundaries due to thermal strain has been proposed.

The techniques of observing dislocations have been gradually developing. Many X-ray diffraction methods have been devised. Noggle and Koehler (20), Kelly and Wei (21), Guinier (22), Lang (23) all used X-ray diffraction in one way or other. The estimations of dislocation densities made by Noggle and Koehler are at best semi-quantitative. The studies

of sub-boundaries (21, 22, 23) raise question as to whether sub-boundaries are completely detectable by the X-ray techniques.

Recently, etching techniques were developed to reveal individual dislocations and established at least an approximate one-to-one correspondence between dislocations and the etch figures. For the high purity zinc used in this experiment, the etching and polishing solutions developed by Vreeland et al. (10) were used.

II. THEORY AND BACKGROUND

In the following, the formation of dislocations and their arrays in the crystals grown from the melt by the Bridgeman technique will be discussed with special emphasis on metallic crystals.

There is an enormous amount of literature published on the subject concerning the sources of dislocations in the crystals grown from the melt. It has been generally accepted that there are five distinct mechanisms for the formation of dislocations. They are:

- 1) propagation of dislocations from a seed onto the growing crystals,
- 2) formation of dislocations due to thermal stress,
- 3) formation of dislocations by vacancy condensation,
- 4) formation of dislocations due to local segregation of impurities that produce a change in lattice parameter,
- 5) dendritic growth.

The last two mechanisms will not be treated here, under the assumption of high purity of the material and of growth conditions under which dendritic growth does not take place.

The theoretical prediction of dislocation formation by vacancy condensation has not been experimentally verified and will not be further considered.

Hence, the first two mechanisms will be treated in the following. General theory will be discussed for a crystal in general, but special emphasis will be made on the metallic crystals grown from the melt.

1) Seed

One obvious source of dislocations is the seed. Whenever a seed crystal contains dislocations which intersect the solid-liquid interface, these dislocations will propagate into the newly forming solid. This is a consequence of the fact that dislocations can only terminate at a free surface, by combining with dislocations of opposite sign, or by closing on themselves.

Dislocations originating from the seed will be introduced into the crystal in two ways as the crystal grows; first by propagation by growth, and second by generation of dislocations by thermal stresses in the seed and propagation of these by growth (5, 18).

Selection of a seed with a preferred crystallographic orientation can improve the crystal perfection in two ways:

a) A seed crystal with "hard" orientation.

Such a seed can raise the critical stress value at which plastic deformation takes place. Thus, the number of plastically generated dislocations during and after the growth will be minimized or eliminated.

b) A seed crystal with a favorable orientation which will allow dislocations to grow out of the crystal.

Dislocations tend to lie on certain crystallographic planes, such as slip planes. Also dislocations and their arrays tend to align themselves along the crystal axis (usually direction of heat flow) at slow growth rate, and along certain crystallographic direction at fast growth rate (5, 14, 16, 20, 21, 24). These properties can be used in selecting the seed such that dislocations can be driven out of the crystal. For example, a seed crystal in which the slip plane makes preferred angle with the crystal axis can be selected. Then the dislocations lying on the slip plane can be driven out of the crystal at fast growth rate. Dash (5) has utilized this principle in growing dislocation-free silicon single crystals.

2) Thermal Stress

The effect of thermal stresses on the crystals grown from the melt is relatively well understood. Billig (36) and Penning (32,33) studied the thermal stresses in Si and Ge in terms of etch pit densities. Such studies in metal crystals have not been studied. Effect of such stresses would be much greater in metal crystals. It is easily understandable that the effects are similar in both types of material, although they differ in extent.

Thermal stresses would be zero if temperature distribution is uniform throughout the entire crystal. This is not generally fulfilled during the growth and the cooling to room temperature. If a non-uniform temperature distribution exists, the displacement of a point in the lattice takes place and may be considered as consisting two parts. One part is due to thermal expansion, the other is the "thermal strain." Thermal strain is the consequence of the fact that displacement due to thermal expansion is not possible without interference with its surroundings. Thermal strain is necessary to keep the different expansions in different parts compatible with each other, if the lattice is to remain continuous.

When the thermal strain is very small, it may be entirely elastic. Beyond a certain critical value, which varies with the type of material and the temperature, thermal strain cannot remain elastic and will be relieved by plastic flow with generation of new dislocations. Furthermore, if plastic deformation takes place to accommodate non-uniform thermal expansion of a crystal, the reverse process will take place when the crystal is brought back to a uniform temperature, say room temperature. Plastic flow will again take place and more dislocations will be generated. In general, however, the proportion of elastic strain will be larger at room temperature because the stress necessary to produce a dislocation increases as temperature decreases.

In metals, the stress necessary to produce plastic flow is usually much lower than in semi-metals. Thus, the dislocation density produced by thermal strain in metal crystals will be even higher than in Si and Ge. This problem has not yet been investigated experimentally.

a) Radial temperature gradient.

If there is radial heat loss from a growing crystal, the shape of the liquid-solid interface would be convex into the solid. Stresses can be introduced in such a crystal, having

temperature variations because of dimensional changes associated with thermal coefficient of expansion. Thus, if the surface is allowed to cool to establish a temperature gradient between the center and the surface, the outer portion of the crystal will tend to shrink, but will be prevented from doing so by the warmer inner core. Accordingly, the surface layers are stretched and the core compressed. If such stresses exceed a critical value, plastic flow takes place and dislocations will be generated.

In the case of low cooling rates the parabolic stress distribution in a simple round bar is represented by the following equations (32):

$$\sigma_z = \left(4 \frac{r^2}{R^2} - 2\right) \sigma_o$$

$$\sigma_\theta = \left(3 \frac{r^2}{R^2} - 1\right) \sigma_o$$

$$\sigma_r = \left(\frac{r^2}{R^2} - 1\right) \sigma_o,$$

$$\text{where } \sigma_o = \frac{1}{8} hR \frac{\alpha E T_o}{1-\nu} \exp \left(-2h \frac{K}{R} t\right)$$

in which h is a constant determining the rate of cooling, T_0 the initial temperature, R the outer radius of the crystal and K the diffusivity of the material.

The stress tensor can be simplified by taking into account the fact that all shear stresses are zero when a hydrostatic pressure is applied. Hence one may subtract from the normal stresses a hydrostatic pressure of magnitude σ_θ as long as plastic flow is concerned.

The two remaining stresses

$$\sigma'_r = \sigma_r - \sigma_\theta \text{ and } \sigma'_z = \sigma_z - \sigma_\theta$$

in radial and axial directions respectively are

shown in Fig. A as a function of r . The net stress giving plastic flow is a radial compression at the surface and an axial compression in the center.

$$\text{Thus, } \sigma'_r = -2 \frac{r^2}{R^2} \sigma_0$$

$$\sigma'_z = \left(\frac{r^2}{R^2} - 1 \right) \sigma_0$$

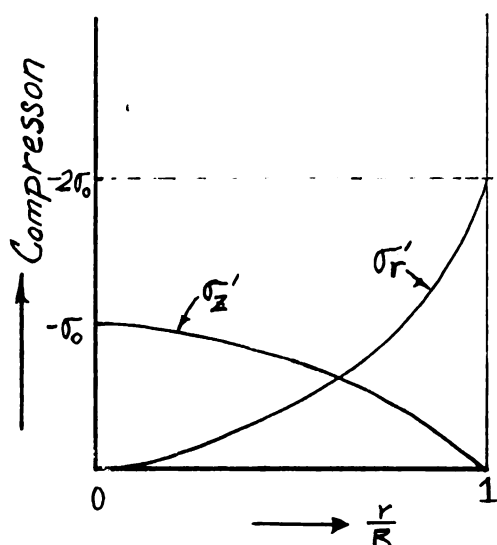


Fig. A

The effective stresses causing plastic flow in the case of radial heat flow.

b) Non-linear axial temperature gradient

A non-homogeneous axial temperature gradient may arise from the radial heat loss. It may also exist in a growing crystal when it is withdrawn quickly during growth.

Under such circumstance, shear strain γ_{rz} may not be zero, where r and z represent the radial and the axial direction, respectively. Such a strain destroys the symmetry of stress pattern with respect to a plane perpendicular to the axis (32, 33). The γ_{rz} can cause a slip non-symmetric with respect to the crystal axis, if a normal stress component, for example σ_z , is present. The γ_{rz} is always accompanied by a z -dependent σ_z as follows directly from the equilibrium condition.

Such stresses and strains are not readily calculated for quenching when a crystal is quickly withdrawn from the melt. Only a qualitative analysis is available to explain the effect of non-uniform axial temperature gradient.

c) Thermal stresses during crystal growth.

In the Bridgeman technique, there are two main sources of thermal stresses during the growth. Radial and non-linear axial temperature gradients will result from (a) a non-zero growth rate, and (b) radial heat loss.

There is no need for further explanations on the radial heat loss. Even if axial temperature gradient $\frac{\partial T}{\partial z}$ were constant in equilibrium condition (before the growth), a term $\frac{\partial^2 T}{\partial z^2}$ will be introduced in the temperature distribution as soon as growth takes place (32).

The stresses induced by these deviations will be minimized when radial heat loss is prevented and the growth rate is slow. Under an ideal condition, the shape of the liquid-solid interface is perfectly planar which implies no thermal stresses are induced.

Formation of Sub-boundaries

Since Frank (14) proposed that suitable networks of dislocations can account for any type of misorientation in any direction between neighboring blocks of mosaic structure, many kinds of substructures have been studied. It is customary to divide these substructures into two categories, depending on their origin and mode of formation. The first category includes the substructures that arise from a particular arrangements of dislocations, which are either formed during or after solidification. The second category includes the substructures arising from a specific distribution of impurities. In the following, only the first category will be treated.

There are two proposed mechanisms by which sub-boundaries can be formed. First, when dislocation density is high enough there is a tendency for dislocations to arrange themselves into two-dimensional arrays forming a system of sub-boundaries (18, 35). At the relatively high temperature prevailing behind the interface, the dislocation mobility would be fairly high. These dislocations, as pointed out by Cottrell (35), would have a tendency to assemble into arrays of dislocations of the same sign, each dislocation lying in a different plane. Faster cooling rates reduce the time during which dislocation mobility is sufficient to permit the formation of sub-boundaries.

The second mechanism was developed first by Frank (29) who suggested the vacancy collapse mechanism to account for the formation of lineage boundaries. As mentioned earlier, this mechanism has not been experimentally verified, and thus will not be treated here.

It is known that thermal stresses are responsible for the formation of sub-boundaries. Washburn and Nadeau (19) observed the complex dislocation arrays were formed locally when the growing crystal was in contact with the crucible wall during the growth. They attributed the formation of the sub-boundaries to the thermal stresses resulting from

different thermal contractions of the crystal and the crucible wall. However, there have been no detailed mechanisms proposed for the formation of sub-boundaries due to the thermal stresses in the crystals grown from the melt.

The formation of the striation type sub-boundaries studied by Chalmers et al. (16, 31) in tin crystals of 99.987% purity was explained in terms of the Frank's mechanism of collapsing vacancy disks. In view of the relatively high impurity content of the material, such an explanation may not be fully justified. The estimated density of the dislocations in the crystals was of the order of 10^8 cm^{-2} .

The work of Noggle and Koehler (20) and of Kelly and Wei (21) on aluminum single crystals grown by the soft-mold technique showed much higher degree of perfection in those crystals. The x-ray estimation of the total dislocation density was of the order of 10^6 cm^{-2} . The misorientation of the sub-boundaries present in the Al crystals ranged from 1 to 20 minutes of arc. Such a high degree of perfection in the crystal might have resulted from low thermal stresses in the soft-mold technique. The radial insulation by the soft-mold material (levigated alumina powder) seems to be directly responsible for the high degree of perfection.

Chalmers et al. (16, 31) have grown striation-free crystals of tin and aluminum. One method is based on the property that the striation width will increase to the comparable dimension of the crystal when the rate of growth and temperature gradient is small enough. Another method used two properties of striations; 1) the dependence of the striation on the crystallographic orientation and the rate of growth of the crystal, and 2) the incubation distance necessary before striations form in those parts of the crystal into which they are not propagated from pre-existing striations. Here they controlled the thermal conditions such that, first, the solid-liquid interface is convex to the liquid, and second, the interface is inclined to the specimen axis.

In the first condition, the convex interface was obtained by a slight radial heat input. At slow growth rates, the striations tend to align themselves with the direction of heat flow, which is normal to the interface. Thus, striations can grow out of the crystal.

In the second condition, the principle is the same as in the first case. Thus, the striations will tend to align themselves perpendicular to the interface if the maximum distance from the interface to the external surface of the crystal is larger than the incubation distance.

It is, however, hard to conceive a crystal free of sub-boundaries when the dislocation density is of the order of 10^8 cm^{-2} . Even when the density is as low as 10^4 cm^{-2} , the randomly distributed dislocations have a tendency to align themselves toward small angle boundaries (18).

III. EXPERIMENTAL

1. Equipments

a) Furnace arrangement.

A modified Bridgeman technique was used in growing zinc crystals of controlled orientation. In this technique, the growing crystal remained stationary in the region between two furnaces where a constant axial temperature gradient was maintained during the growth. The crystal growth consisted of three stages of operation; soaking, solidification, and subsequent cooling to room temperature.

Two type MK-1004-S Hevi-Duty electric furnaces were vertically mounted with a separation of 1-1/2" between them. A zirconia tube with an inside diameter of 1-1/4" was inserted vertically into the furnaces. The gap between the two furnaces was insulated with spun fiber glass. The schematic drawing of the furnace arrangement is shown in Fig. 1. The actual furnace arrangement is shown in Fig. 5.

A general view of the instrument panel is shown in Fig. 6. All the control instruments used were manufactured by Minneapolis-Honeywell Company. The upper furnace temperature is controlled by a model SY153R10 recording controller. An axial temperature gradient can be maintained by setting the

corresponding temperature difference on the set point unit (model 62-R-100-D). Any deviation from the difference is indicated in the deviation amplifier (model 62-R-237-A).

The recording controller features two modes of operation; soaking and program cooling. A desired soaking period (0-6 hours) can be set at a desired temperature setting. After the soaking period, program cooling takes place linearly at a desired rate, while a constant temperature difference is maintained between the two furnaces. The span of program cooling can be changed. Most of the crystals have been grown with the span of 10 millivolts, corresponding to a temperature range of 250 degree centigrade.

Fig. 1 also shows the position of the crucible and the internal arrangements. The crucible is suspended by alumel wire in a position such that the bottom 1" of the specimen is in the lower furnace and the top 1-1/2" is in the upper furnace. In the crucible, two thermal blocks T_1 and T_2 are in contact with the two ends of the specimen. Thermocouples are placed near the T_1 and T_2 blocks thus establishing an axial temperature gradient. Crucibles A and B in Fig. 2 were made of graphite and can be split vertically into halves in order to minimize mishandling of the grown crystals during the unpacking process. The dimensions of the crucibles

are given in Fig. 2. The soft-mold material is alumina powder (500 mesh) mixed with about 2 wt per cent of graphite powder. The mixture is tamped around the zinc charge and the thermal block T_1 .

An inert atmosphere in the furnace tube was provided by having a continuous flow of dry nitrogen. Furthermore, carbon was mixed in the mold material to provide a deoxidizing atmosphere.

b) Acid String Saw

An acid string saw shown in Fig. 7 was used to cut the grown zinc crystals without introducing any mechanical stresses. Nitric acid (about 40%) was used and its delivery was made by means of Saran string. A 6 rpm Bodine electric motor drives a 2-1/2" long crank arm. One end of the Saran string is attached to the crank arm and a weight is attached to the other end to give some tension to the thread. The string is guided by narrow grooves in the middle of the faces of round spools, two of which are immersed in the nitric acid bath. In order to make a better delivery of the acid, the string is doubly laid.

The cutting speed depends on the acid concentration and the amount of the acid delivered by the Saran string.

2. Experimental Procedure

The material used in growing the crystal specimen is 99.9994% purity zinc obtained from New Jersey Zinc Company. It was obtained in the form of round rod of 3/8" in diameter. The round rod was rolled and machined to the standard sample dimensions given in Fig. 3a. The bottom 1" of the specimen can be replaced by a seed of known orientation. The seed was welded to the specimen with an acetylene torch or a gas torch using ammonium chloride as a flux. Before and after the welding, the surface of the specimen was cleaned by immersing it in dilute hydrochloric acid.

The specimen was then placed in the small conical hole in the center of the top face of the thermal block T_2 . The alumina powder mixture was tamped around the specimen, the top face of which was in contact with the thermal block T_1 . The packed crucible was then suspended by alumel wire, so that the bottom 1" of the specimen was in the lower furnace and the top 1-1/2" was in the upper furnace.

The furnace was preheated to the desired temperature before placing the crucible into the furnace tube. Next, the charge was soaked for some hours to obtain a temperature distribution as uniform as possible. At the end of the soaking

period, the charge was program cooled linearly at a given rate, while maintaining the constant axial temperature gradient.

Typical growth settings are as follows:

Upper furnace temperature	475°C
Lower furnace temperature	355°C
Soaking period	3-1/2 hrs.
Growth rate	1 mm/min.

At the typical settings, the standard sample has the trace of the liquid-solid interface in the seed at $1/2 \pm 1/8$ " from the bottom end of the sample. The trace of the interface indicates the demarcation line above which the sample has been molten during the soaking period. The trace is easily visible to the naked eye.

The grown sample was etched in concentrated hydrochloric acid. Visual examinations of the etched surfaces were made to determine if there are visible sub-boundaries. The crystal was then cut by means of the acid saw to dimensions convenient for subsequent microscopic examinations. Some difficulties were encountered in obtaining a flat surface by the acid saw. All the samples were cut to reveal the surfaces nearly parallel to $\{10\bar{1}0\}$ type planes.

The samples were glued to plexiglas (acrylic plastic) plates (1/10" thick) of appropriate size with plastic adhesive. Subsequent handling of the sample was done entirely by handling the plastic plate.

The sample was next etched to reveal dislocations on $\{10\bar{1}0\}$ surfaces. Metallographic examination was made on Bausch and Lomb Research Metallograph, and photomicrographs were taken using standard techniques.

Polishing and Etching of Dislocations

Present experiment requires polishing and etching solutions which are suitable for undecorated high purity zinc single crystals. It has been found that the solutions developed by Vreeland et al. (10) were suitable for the purpose. The solutions are:

P-1	160 gr CrO_3 20 gr Na_2SO_4 500 ml distilled water
P-2	Equal parts of: Methanol 30% H_2O_2 conc. HNO_3
P-3	160 gr CrO_3 500 ml distilled water

E	One part:	1 gr $\text{Hg}(\text{NO}_3)_2$
		1 ml conc. HNO_3
		500 ml H_2O
	Two parts:	distilled water

The polishing procedure:

1. Dip with mild agitation in solution P-1 for 20-100 sec.
2. Dip occasionally in solution P-2 to accelerate the polishing process.
3. Dip finally in solution P-2 to remove the CrO_3 film.

The etching procedure:

1. Dip with mild agitation in solution E, 5-6 sec.
2. Dip with mild agitation in solution P-1, 5-6 sec.
3. Dip with mild agitation in solution P-3, 2-3 sec.
4. Rinse in running tap water.
5. Rinse in running distilled water.
6. Dry in an air blast.

Best results are obtained when the polishing procedure is immediately followed by the etching procedure.

The formation of etch pips is due to the rapid diffusion of mercury to dislocation sites over the polished surface, and the diffused mercury retards the rate of polishing.

In order to verify the validity of the etching technique, a series of experiments was made. The results were in complete agreement with the qualitative observations of

the dislocation etch patterns made by Vreeland et al. This may be considered to be sufficient evidence to make quantitative observations meaningful, since Vreeland et al. have established one-to-one correspondence between the etch pips and the dislocations by the same etching technique.

Using the etching technique, a study of distributions of dislocations and sub-boundaries was made. Various sections of the grown crystals were etched and the etch patterns, as revealed on $\{10\bar{1}0\}$ planes, were studied. The samples of orientation 2-1 were studied on cross-section surfaces perpendicular to the growth direction. The samples of orientation of 1-1 were cut to expose the cross-section surfaces making an angle of 30° with the horizontal cross-section. In the later case, the side surfaces $(01\bar{1}0)$ parallel to the growth direction were also observed with or without cutting by acid. In the Fig. 4, the observed surfaces of the samples of orientations 1-1 and 2-1 are cross-hatched with red color.

Surfaces parallel to $\{10\bar{1}0\}$ planes in the samples of different orientations were cut and observed similarly. Such surfaces were cut carefully so that exposed surfaces were within $\pm 1^\circ$ of the crystallographic planes of $\{10\bar{1}0\}$ as determined by the X-ray back-reflection method. The back-

reflection technique may have an uncertainty of $\pm 2^\circ$ in itself. Thus the maximum angular deviation was $\pm 3^\circ$ from the $\{10\bar{1}0\}$ plane. Vreeland et al. have shown that good etch patterns can be obtained on the surfaces making an angle as large as 5.5° from the prism plane. They have also shown that etch pips were observable on the surface as much as 15° from the prism plane. Therefore it is quite allowable to deviate as much as $\pm 3^\circ$ from the prism plane, so far as etching of dislocation is concerned.

A series of experiments was carried out in order to improve the crystal perfection. Emphasis was placed on 1) minimizing the thermal stress during and after the growth by minimizing the radial heat loss, 2) preventing the propagation of sub-boundaries from the seed by the offset method. In the following, these will be discussed further.

Reduction in Radial Heat Loss

a) By a conduction sleeve with external insulation around it.

The purpose of installing the conduction sleeve around the entire length of the crucible is to improve axial heat conduction, thus to reduce the radial heat loss. The radial heat loss will be further reduced if the conduction sleeve is effectively insulated. Steel plate of thickness 0.1"

was wrapped around the furnace tube. The 6" steel sleeve was long enough to cover the whole length of the crucible. The insulation was done by wrapping the portion of the furnace tube between the upper and lower furnaces with spun fiberglass.

The combination of the conduction sleeve and the insulation should result in a greatly reduced radial heat loss and an increased uniformity in the axial temperature gradient.

b) By increasing the crucible size.

By increasing the crucible size, the thickness of the insulating alumina mixture is increased. Two crucibles A and B whose dimensions are given in Fig. 2 were used using specimens of the same size. The thickness of the alumina insulation in the crucible B is about twice that of the crucible A.

The effects of (a) and (b) were studied in terms of dislocation density and sub-boundary distribution.

Elimination of Sub-boundaries - Offset Method

The purpose of the offset method is to prevent the propagation of sub-boundaries from the seed. The technique of eliminating the sub-boundaries is to make them grow out to free surfaces. This is possible, since the sub-boundaries

tend to align themselves along the growth direction at slow growth rate.

Zinc specimens were machined in the shape shown in Fig. 3b. The "S" shaped constricted portion is such that no vertical straight lines can be drawn on the flat surface from the seed without crossing free surfaces.

In Fig. 3b, the sub-boundaries running in the direction perpendicular to the flat surface, would be eliminated provided they grow in the direction parallel to the growth axis. The crystal grown in this manner would be free of the sub-boundaries running perpendicular to the flat surface. But the sub-boundaries running parallel to the flat surface would still remain in the crystal. Now a seed was obtained from the crystal. But the seed was rotated 90° about the specimen axis and welded to another offset sample which was subsequently grown.

Now the remaining sub-boundaries would grow out to free surfaces, thus leaving the second crystal free from sub-boundaries propagating from the seed.

This offset method can be used more than once to insure a crystal free from the sub-boundaries propagating from the seed.

It must be noted that the offset method would be most

effective in eliminating the sub-boundaries only if there are no newly formed sub-boundaries during the growth. However, one must concede a possibility of sub-boundary formation by rearrangements of the randomly distributed dislocations, so long as the dislocation mobility is not zero.

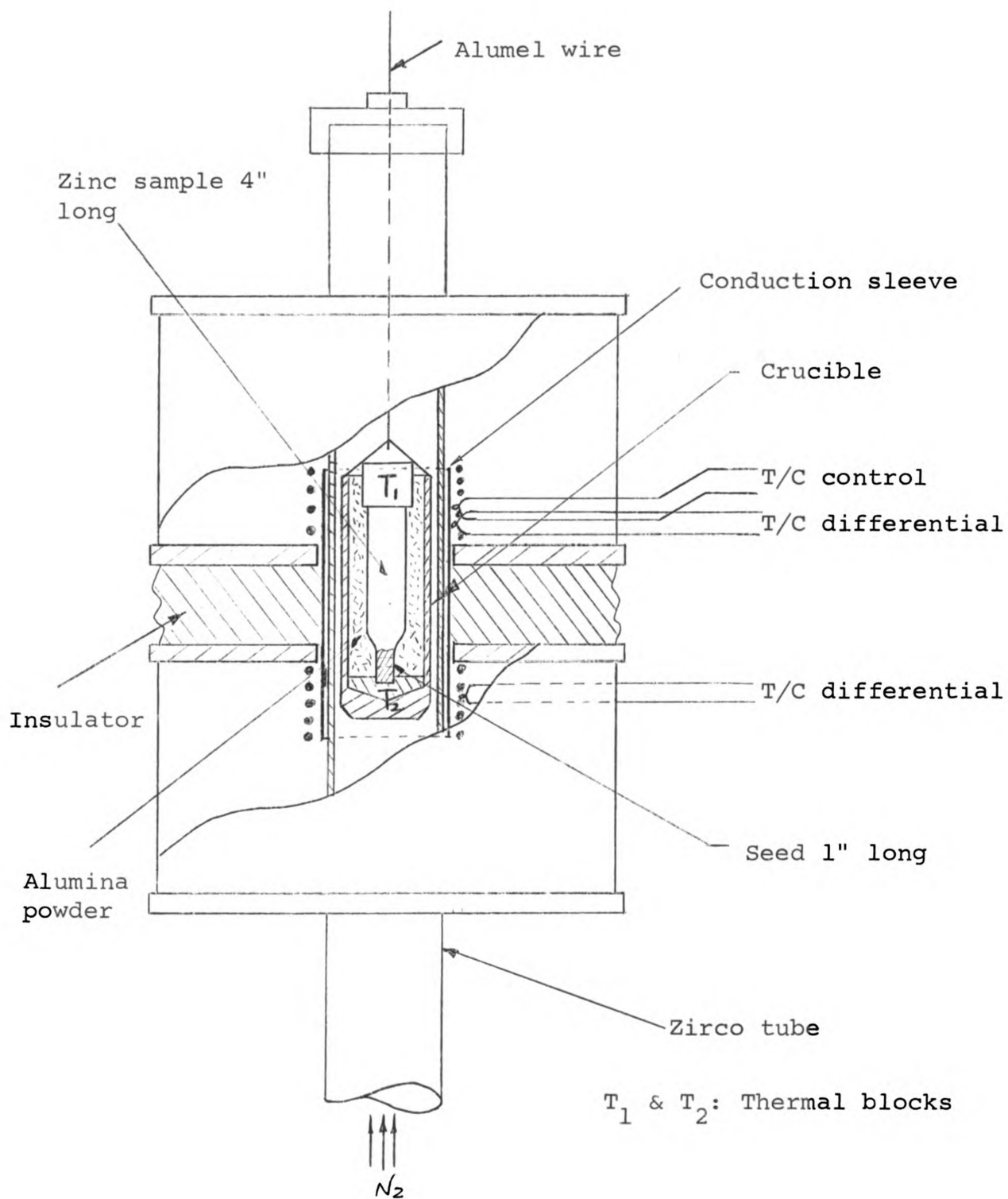


Fig. 1. Furnace setup (schematic)

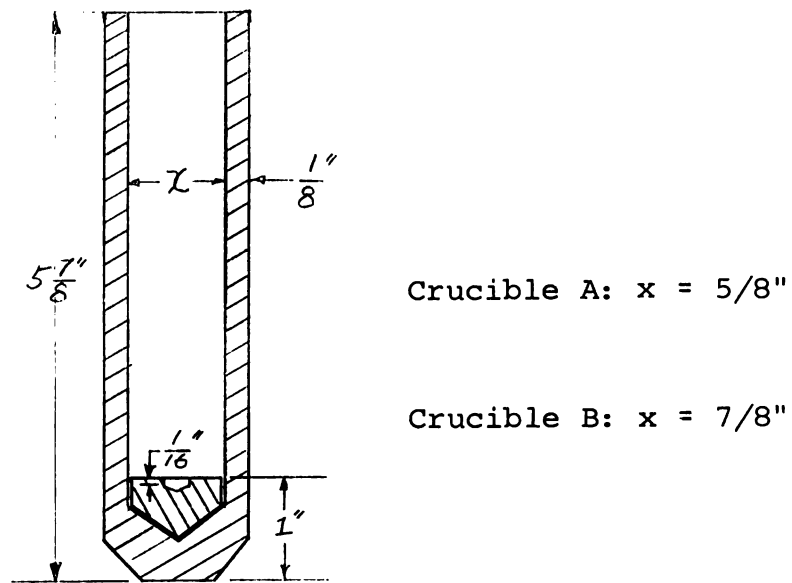


Fig. 2. Crucible design.

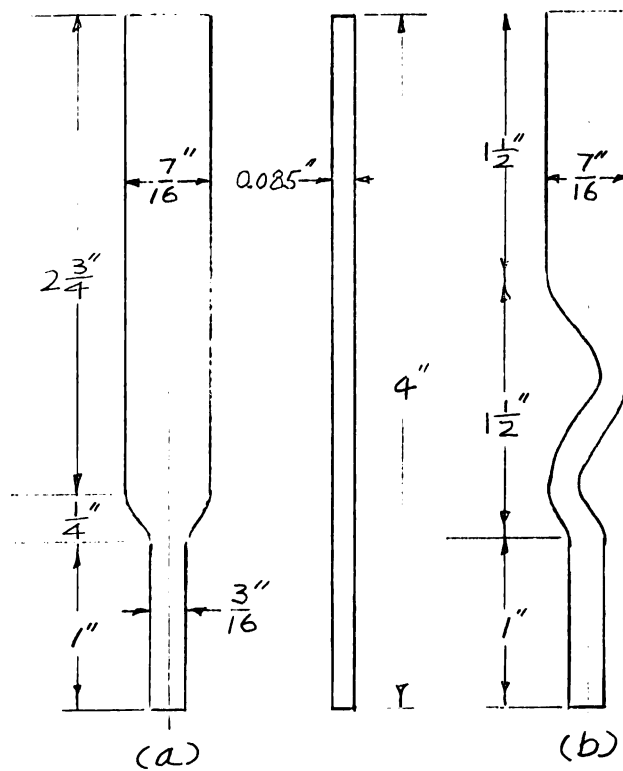


Fig. 3 (a) Standard specimen.
(b) Offset specimen.

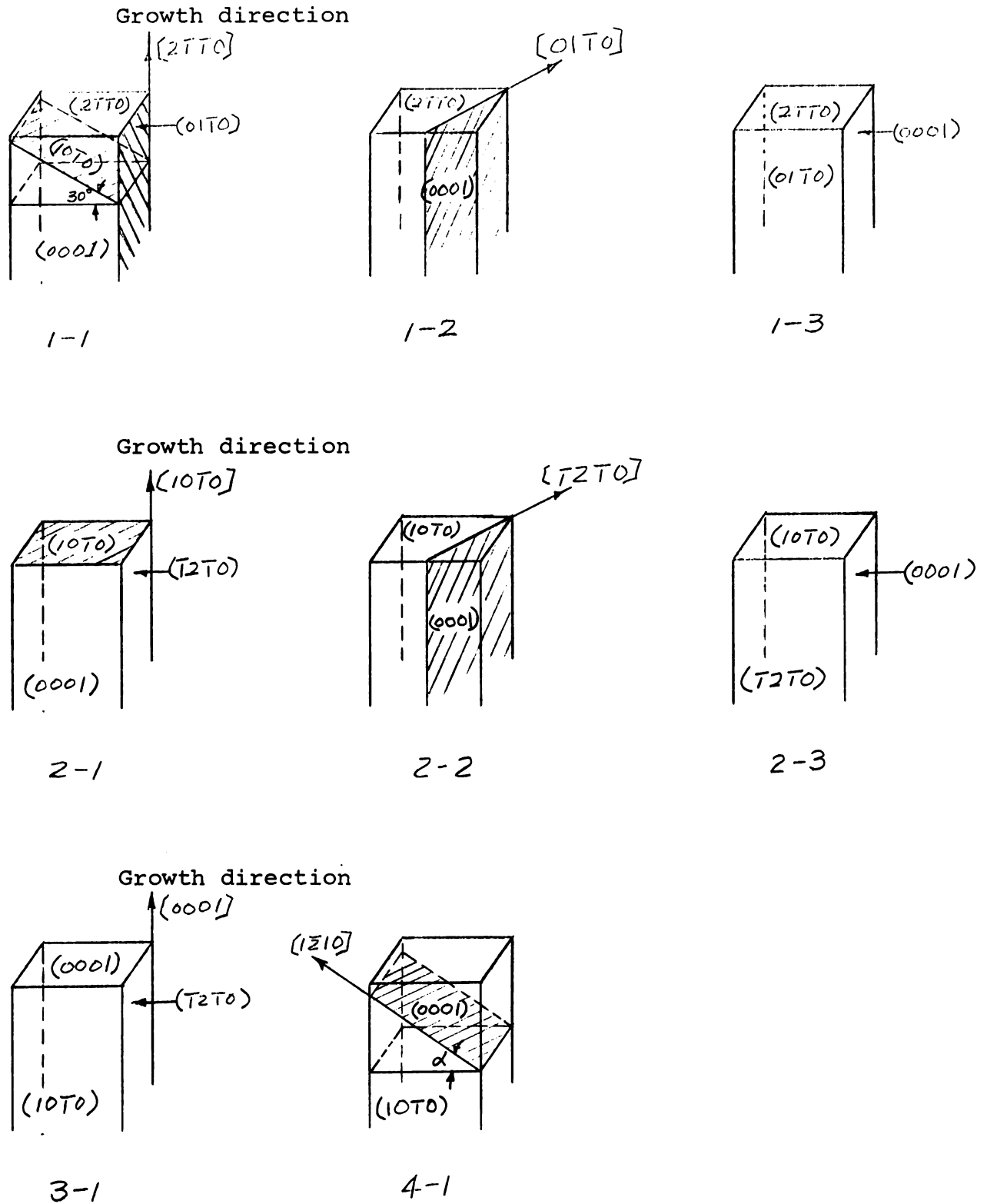


Fig. 4. Orientations of the crystals and the seeds and their designations.

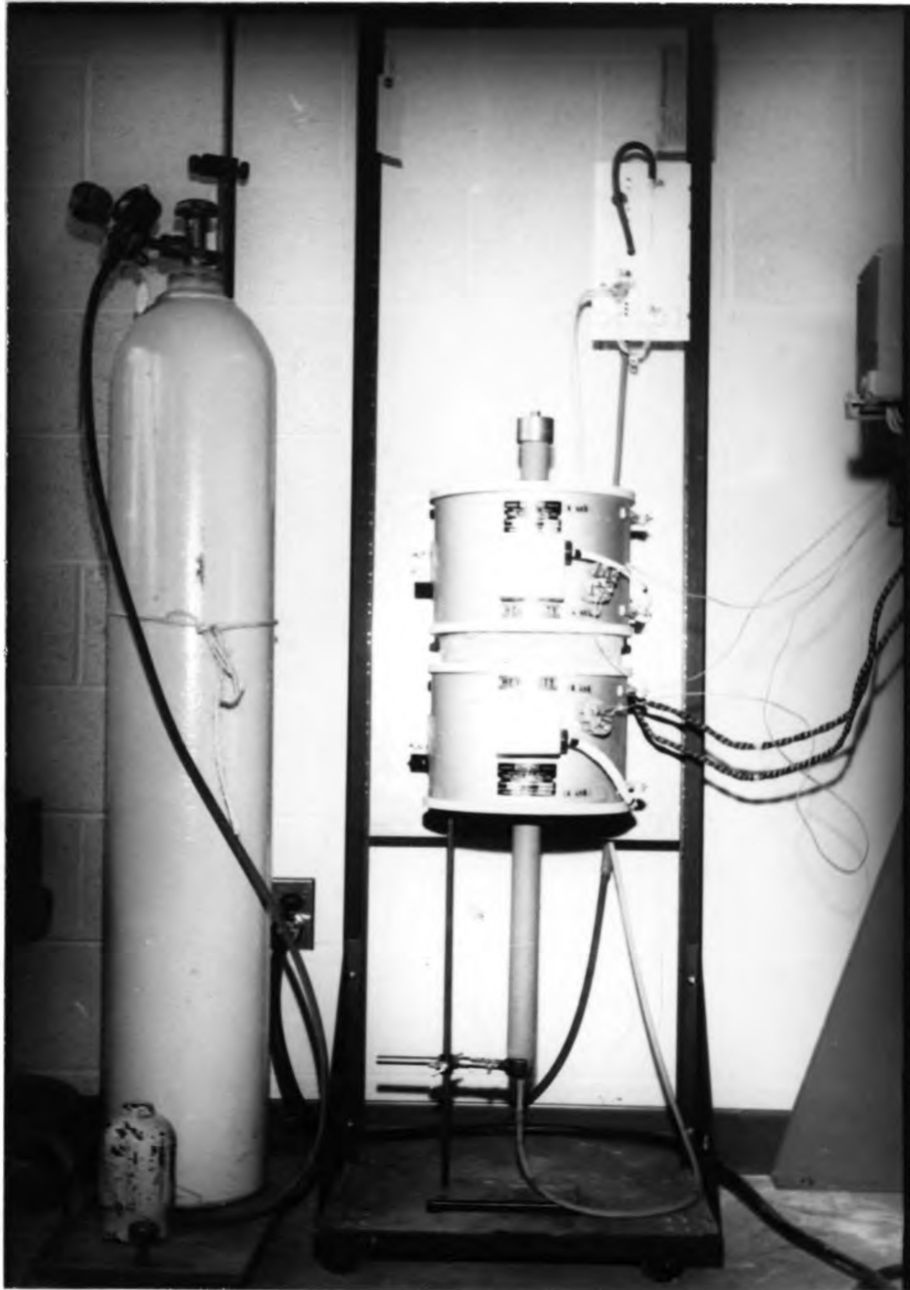


Fig. 5. Furnace setup.



Fig. 6. Furnace control panel.

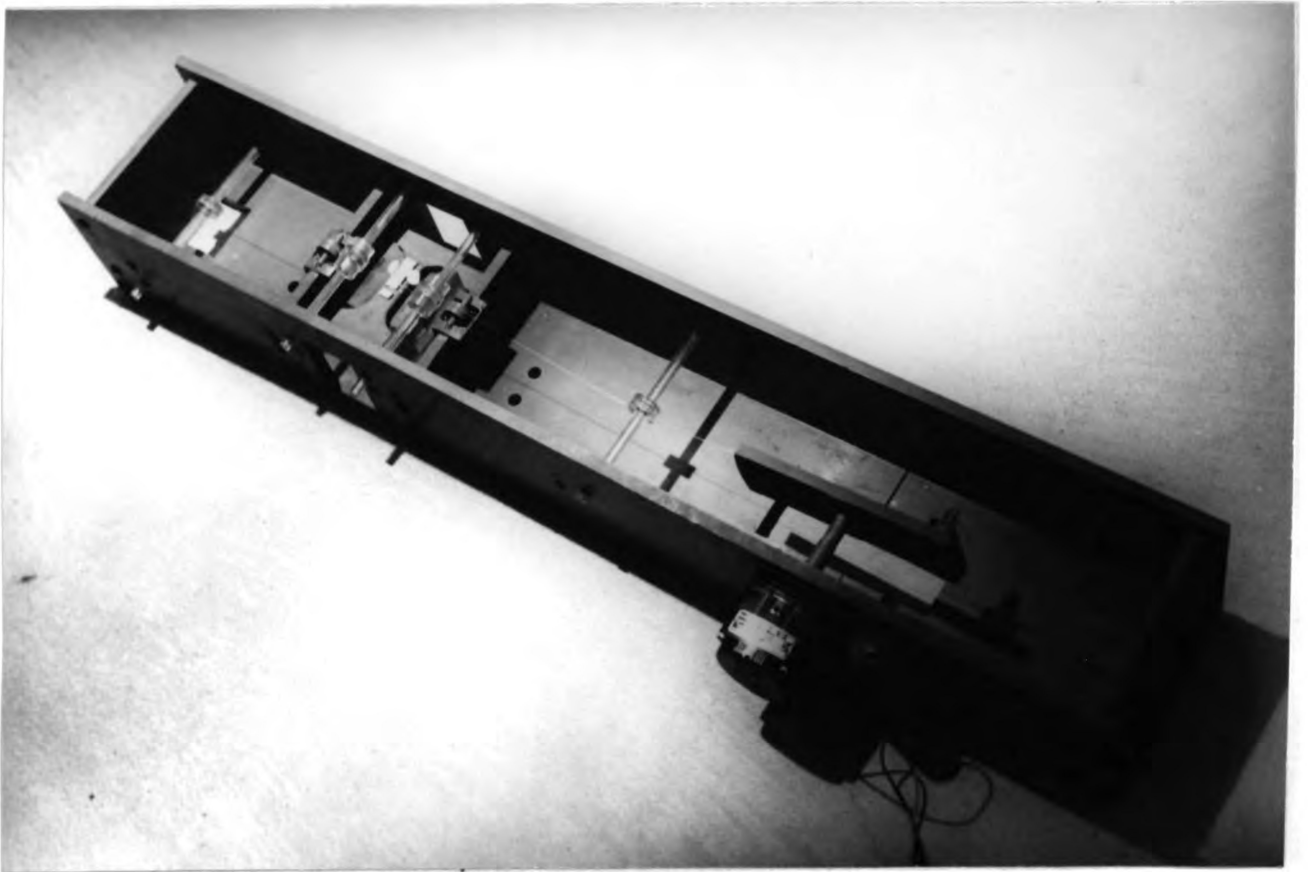


Fig. 7. Acid string saw.

IV. RESULTS AND DISCUSSION

In the following, the results of the metallographic inspection of the zinc single crystals will be discussed in terms of the photomicrographs of the dislocation etch figures as revealed on the prism plans.

Before any attempts were made for the improvement of the perfection of the crystals, a study was made on the distributions of dislocations and sub-boundaries in the crystals. The results of the study are summarized in Figs. 8 through 13.

The etch patterns, shown in Figs. 8 and 9, show that the sub-boundaries tend to align themselves such that their traces in the $\{10\bar{1}0\}$ plane are along the crystallographic directions of $\langle 2\bar{1}\bar{1}0 \rangle$ and $\langle 0001 \rangle$. Generally speaking, the sub-boundaries running in the direction $\langle 0001 \rangle$ have greater tendency to be straight, as shown in Fig. 9. These sub-boundaries are usually interconnected by means of short, but almost perpendicular branches. It can also be observed that the $\langle 2\bar{1}\bar{1}0 \rangle$ direction is immediately identifiable, since the etch pips are elongated in the direction, showing the crystallographic symmetry.

Along the relatively large angle boundaries, the dislocation etch pips are overlapped. It is extremely difficult

to resolve or to count individual pips along such sub-boundaries.

When such sub-boundaries are present, an uncertainty arises in the expression of the degree of perfection of the crystal in terms of dislocation density. Elimination of such boundaries not only improves the perfection of a crystal, but also the perfection can be expressed more accurately and meaningfully.

Fig. 10 shows sub-boundaries aligned nearly in $[2\bar{1}\bar{1}0]$ direction in a sample with the orientation 2-1. In order to determine whether they have grown from the seed, samples with the orientation 2-2 and 2-3 have been grown from seeds obtained from the sample 2-1. The seeds were rotated 45° and 90° about the growth direction and welded to the standard zinc specimens to grow the sample 2-2 and 2-3, respectively. The sample 2-2 was then examined on the horizontal cross-section and is shown in Fig. 11. One large sub-boundary has been retained and makes an angle of about 45° with the cross sectional edges, indicating it is still running nearly in $[2\bar{1}\bar{1}0]$ direction. There are no sub-boundaries parallel to the cross sectional edges throughout the observed surface. A further evidence can be shown similarly when a crystal of the orientation 2-3 was

examined. Here sub-boundaries (not shown) are still running in $[2\bar{1}\bar{1}0]$ direction as well as $[0001]$ direction.

This clearly indicates the sub-boundaries are propagating from the seed. Therefore, if such sub-boundaries were to be eliminated from a grown crystal, they must be prevented from growing into the crystal from the seed.

Next, several samples of the orientation 1-1 have been observed on the cross-section $(10\bar{1}0)$ and the side faces $(01\bar{1}0)$. The cross-section makes an angle of 30° from the horizontal cross-section. The side surfaces were observed in as-grown as well as acid-cut conditions.

Background density of dislocations in the cross section surface $(10\bar{1}0)$ is of the order of $7 \times 10^4 \text{ cm}^{-2}$ (ranging from $5.6 - 8.0 \times 10^4 \text{ cm}^{-2}$), while that of the side surface $(01\bar{1}0)$ is about $2 \times 10^4 \text{ cm}^{-2}$ (ranging from $1.5 - 2.4 \times 10^4 \text{ cm}^{-2}$). Thus the dislocation density in the cross sectional surface is about 4 times that in the side surface. In some cases, the difference is as much as one order. Fig. 12 shows the typical background densities of the two surfaces, as revealed on $(10\bar{1}0)$ planes of the sample with the orientation 1-1. In these photomicrographs, there is a difference of a factor of about 4 in the dislocation densities. This particular crystal is one of the improved crystals, but similar

observations can be made for unimproved crystals.

More striking differences are observable in the sub-boundary distributions. Far greater numbers of sub-boundaries are observable on the cross-section than the side face where a few sub-boundaries are observable occasionally. The reason for this can be seen in Fig. 13. The sub-boundary labeled P in both photomicrographs is the same one. But it is hardly recognizable in Fig. 13b.

These observations of differences in dislocation densities and number of sub-boundaries in the two surfaces suggest that most of the dislocation lines grow parallel to the growth direction. This is a qualitative agreement with the observations made on the melt-grown single crystals (20, 21). Noggle and Koehler found that the number of sub-boundaries parallel to the growth direction is on an average three times those perpendicular to the direction. Kelly and Wei also found that dislocation lines run parallel to the growth direction.

In view of these facts, it would be misleading to determine the dislocation density by observing $\{10\bar{1}0\}$ planes parallel to the growth direction.

1) Reduction in Radial Heat Loss

a) Effect of the conduction sleeve with external insulation around it.

Changes in the background dislocation densities in the crystals grown in crucible A have been studied before and after the installation of the conduction sleeve and the insulation. Before the installation the background densities varied considerably from one place to another, ranging from 1 to $5 \times 10^5 \text{ cm}^{-2}$. This value is roughly in agreement with the reported values of dislocation densities of Zn single crystals grown by Bridgeman technique (10, 37).

After the installation, distribution of the background dislocations became more uniform and the densities were consistently about $5-7 \times 10^4 \text{ cm}^{-2}$. This is a reduction in the dislocation density as much as one order. Furthermore, the deviations from the average value are much smaller due to the uniformity of the background dislocations. Consequently, the average values became more meaningful and thus more representative, so far as the background dislocation density is concerned.

However, the effect on sub-boundary formation is not immediately noticeable. This subject needs more experimental data to conclude if there is any effect.

b) Effect of the crucible size.

From studies with the original Bridgeman furnace, it was learned that zinc single crystals can be grown consistently only when the minimum clearance between the wall and the crystal exceeds about $1/16$ of an inch. Since the alumina mixture is packed between the crucible wall and the charge, the larger clearance implies greater insulation on account of the soft-mold material.

Crucible A was able to grow consistently single crystals of $7/16$ " x 0.1 " in its cross-section. In this case, the clearance is about $1/8$ ". For a charge of the same size, crucible B provides a clearance of about $1/4$ ".

Several single crystals grown in crucible A under the growth of a temperature gradient of 10° C/cm and a growth rate of about 1 mm/min. were examined. The cross sections show large numbers of sub-boundaries, which were not propagated from the seed, near the corners. Such sub-boundaries are nearly parallel to both edges of the cross section, as shown in Fig. 14a. Their appearance is quite different from those which have been propagated from the seed.

Next, another crystal of the same size was grown in crucible B in which the thickness of the insulation is about twice as much. The growth condition was the same as before.

When this second crystal was examined, there were no such sub-boundaries as in the case of crucible A. Fig. 14b shows a similar corner of the cross section of the sample grown in crucible B.

The exact mechanism of formation of such sub-boundaries is not clear. But it is quite obvious that thermal stress is responsible for the formation. The greater insulation in crucible B apparently reduced the radial temperature gradient, and hence the thermal stress, to a sufficient extent to prevent the formation of sub-boundaries near the corners.

It is not immediately noticeable if there is any improvement in the background density.

2) Elimination of Sub-boundaries by the Offset Method

Several samples with orientations of 1-1 and 1-2 were grown by the offset method and the etched surfaces $(10\bar{1}0)$ were observed as usual. It has been found that the following procedure is most effective in eliminating the sub-boundaries in both directions.

The procedure:

- i) Use a seed with orientation 2-1 to grow a crystal of orientation 2-3 with offset.

- ii) Obtain a seed with the orientation 2-3 from the grown crystal.
- iii) Use the seed (the orientation 2-3) to grow a crystal of the orientation 2-1 with offset.

By procedure i, the sub-boundaries running in $[2\bar{1}\bar{1}0]$ direction have been effectively, but not completely eliminated. The sub-boundaries running in $[0001]$ direction and some short segments of sub-boundaries running in $[2\bar{1}\bar{1}0]$ direction were retained. Examinations on the cross-section surfaces of the "S" shaped constricted region were made on the bottom portion and the top portion of the "S" region. The surfaces in the bottom portion revealed that there are sub-boundaries running all the way across the surface in the $[2\bar{1}\bar{1}0]$ direction. Sub-boundaries in the top portion are short segments running in the $[2\bar{1}\bar{1}0]$ direction near the free surfaces, indicating the sub-boundaries running all the way across the surface have been eliminated by the offset.

The retained sub-boundaries running in the $[0001]$ direction in the crystal of orientation 2-3 are usually localized to one side of the crystal, leaving the other side substantially low in the number of such sub-boundaries. The region of low sub-boundary density is sometimes large enough to cut a seed of $1/4$ " in width. The seed obtained

in this way has the orientation 2-3 and was used to grow the crystal of orientation 2-1 with offset. This process eliminates the sub-boundaries running in the $[0001]$ direction.

The crystals grown in this manner are substantially free from sub-boundaries, except some short segments of polygonized sub-boundaries. The linear density of dislocations along the polygonized sub-boundaries is of the order $1-5 \times 10^3 \text{ cm}^{-1}$. The disorientation ranges from 5 sec. to 30 sec. Most of the sub-boundaries have a disorientation of about 10 sec. The average distance between the sub-boundaries is about 2 mm. In some cases, it is as large as 3.5 mm. In Fig. 15, a cross sectional surface $(10\bar{1}0)$ of the crystal of orientation 1-1 is shown. Some difficulties in focusing the whole cross section were encountered in the central region. This is due to the fact that acid-cut surface is not perfectly flat. Nevertheless, some traces of sub-boundaries can be seen even in the dark region and there are no larger sub-boundaries than ones in the bright region. The disorientation of the sub-boundaries labeled P_1 is about 10". That of P_2 is about 25". There are some sub-boundaries aligned nearly in the $[2\bar{1}\bar{1}0]$ direction. The disorientation of the P_3 is about 5". The amount of sub-boundaries running the $[2\bar{1}\bar{1}0]$ direction is negligible compared to the polygonized sub-boundaries.

The sub-boundaries P_4 and P_5 are not clearly defined. Large numbers of dislocations are concentrated along the arrays. It seems as if the dislocations are in the process of forming more clearly defined sub-boundaries. If sufficient time were given by slower growth rate, the percentage of such sub-boundaries (P_4 and P_5) would decrease because the concentrated dislocations would align themselves toward more clearly defined arrays. At faster growth rate of 2 mm/min., the sub-boundaries become more diffused and the background density increases somewhat. Fig. 16 shows some typical cases.

It is interesting to note that the polygonized sub-boundary increases in its disorientation as it traces from the interior to the free surface. This is the general case, as can be observed in the sub-boundaries P_1 , P_2 , P_4 , and P_5 . The central region of the crystal is almost free from sub-boundaries.

Somehow, the dislocations near free surface seem to have higher mobility than those in the inner portion of the crystal. This may be so because the thermal stresses, which reach the maximum values at the free surface, would serve as the driving force for the climb or the simple glide of dislocations or both. The driving force would be greater for

the dislocations near the surface, thus resulting in greater amount of polygonization. It is difficult to say which mechanism, climb or simple glide, is operating.

If the thermal stresses are responsible for the formation of such polygonized sub-boundaries, a sufficient reduction in the thermal stresses during the growth should prevent the formation of such sub-boundaries. This would be an interesting and worthwhile topic to be investigated further.

The average length of the polygonized sub-boundaries is about 0.6 mm/mm^2 or 6 cm/cm^2 . Since the linear density of dislocations in the sub-boundaries ranges from 1 to $5 \times 10^3 \text{ cm}^{-1}$, the dislocation density due to the sub-boundaries would be in the range of $6\text{--}30 \times 10^3 \text{ cm}^{-2}$. The observed total dislocation density is about $6\text{--}9 \times 10^4 \text{ cm}^{-2}$.

This is about one order of improvement over the crystals grown at the beginning of this work. Moreover, this is a substantial improvement over the densities reported in the literature. Vreeland et al. (10) have reported the density of $1\text{--}10 \times 10^5 \text{ cm}^{-2}$ in high purity zinc crystals grown by the Bridgeman technique. Noggle and Koehler (20) have reported the density of the order of 10^6 cm^{-2} in the aluminum crystals grown by the soft-mold technique.

The value of sub-boundary disorientations in Al crystals grown by the soft-mold technique, reported by Kelly and Wei ranges from 1' to 20' of arc, as determined by the micro-focus X-ray technique of Schultz. In this work, the value has been improved to about 5" to 30" of arc in the best crystals.

The etching technique is capable of measuring the disorientations up to 30" rather accurately at a magnification of 100 x. It would be of interest to examine the crystals grown in this work by a sensitive X-ray technique in order to confirm, at least qualitatively, the results obtained by the etching technique.

Figs. 17 and 18 show the pseudo Kossel patterns of crystals Y and C, respectively. Both crystals have the same orientation 2-1, and the patterns were taken with the x-ray beam perpendicular to the basal plane. The x-ray target was copper and a nickel filter was used. The exposure was the same in both cases. Crystal C was grown from a seed crystal of orientation 2-3 and the offset method was used. Crystal Y was grown from a seed 2-1 without the offset.

The pseudo Kossel lines are very sensitive to any deviation from perfect crystal (53). Such imperfections

are indicated by an increase in intensity, or a displacement of the pattern as a whole. Sometimes many types of discontinuities, such as gaps, overlaps and local line-shifting, are observable in the pattern due to the imperfections. The sub-boundaries between slightly disoriented regions are indicated by gaps if they form ridges on the surface, or as overlaps if they form valleys. Local lattice rotation is sometimes registered on the film as local line-shifting of the pseudo Kossel pattern, depending on the axis of rotation.

Fig. 17 shows many discontinuities which arise due to the presence of the corresponding sub-boundaries at which the Bragg condition of reflection is not satisfied. The size of the gap, overlap, or line-shifting, represents the size of the sub-boundary disorientation. The doublets are due to the K_{α_1} and K_{α_2} . A close examination reveals the following:

- (a) There are large numbers of discontinuities in the pattern of crystal C, represented mostly by gaps and line-shiftings, especially in the circular rings which correspond to the basal plane. In contrast, there is no such observable discontinuity in the pattern of crystal C. This clearly indicates that crystal C does not contain such large sub-boundaries as in crystal Y.

- (b) Most of the images of sub-boundaries in the pattern of crystal Y intercept the Kossel lines vertically, indicating that they are aligned along the growth direction. The difference of orientation between neighboring subgrains is a rotation of about 10° about an axis nearly parallel to the growth direction.

This supports the previous observation made by the etching technique that most of the sub-boundaries tend to run nearly parallel to the growth direction.

- (c) Despite the fact that the x-ray patterns were taken under the condition of same exposure, the reflection lines of the crystal Y are much stronger and broader. This is a further proof that the crystal C is much higher in the lattice perfection than the crystal Y.

A reasonable estimation shows that sub-boundary disorientations of about 1° of arc can be detected in the x-ray pattern of crystal C. This value may be as high as several minutes of arc in case of the crystal Y due to the stronger and broader reflection lines. The largest gaps found in the pattern of crystal Y correspond to about 20° of arc.

Along the reflection lines in the pattern of the crystal C, some localized intensity variations can be observed. This may well be due to the localized imperfections in the

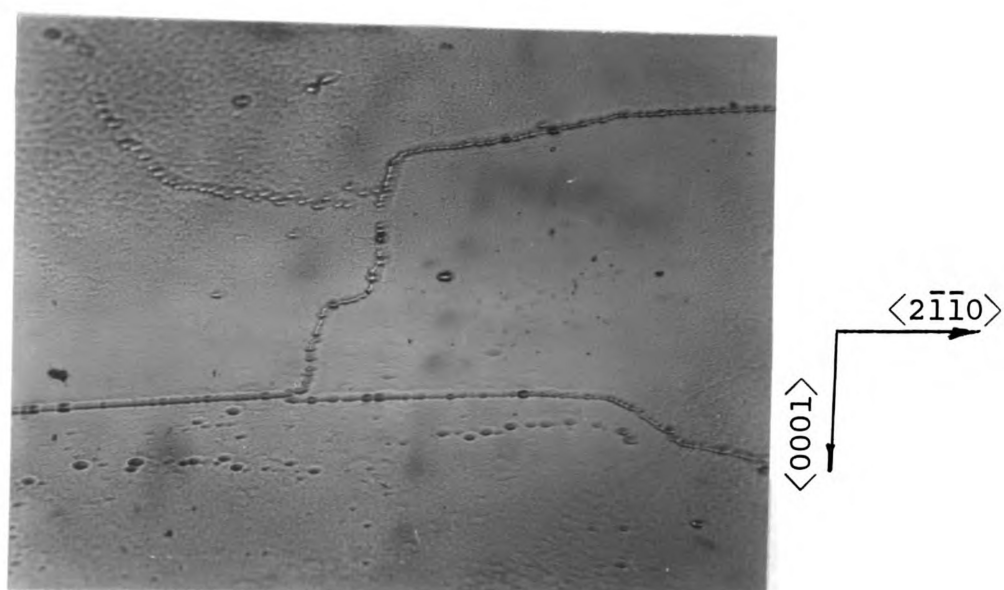
corresponding crystallographic planes. The imperfections could be very small angle boundaries or even some dislocation lines. It is difficult to say which of the two types of imperfections are responsible for such intensity variations. The Schultz technique can be used for the study of such imperfections in greater detail.

All in all, the x-ray patterns of the crystals Y and C prove that the offset method, when properly employed, is capable of eliminating the large sub-boundaries which propagate from the seed, thus resulting in crystals substantially free from sub-boundaries. This supports the previous observations made by the etching technique.

In summary, Table I shows all the grown crystals and the results of microscopic examination of the crystals. The axial temperature gradient is about 10° C/cm for all the crystals. Crystals no. 31 and 33 are the best crystals and they are substantially free from sub-boundaries. The cross sectional prism planes of the crystals are shown in Figs. 15 and 16, respectively.

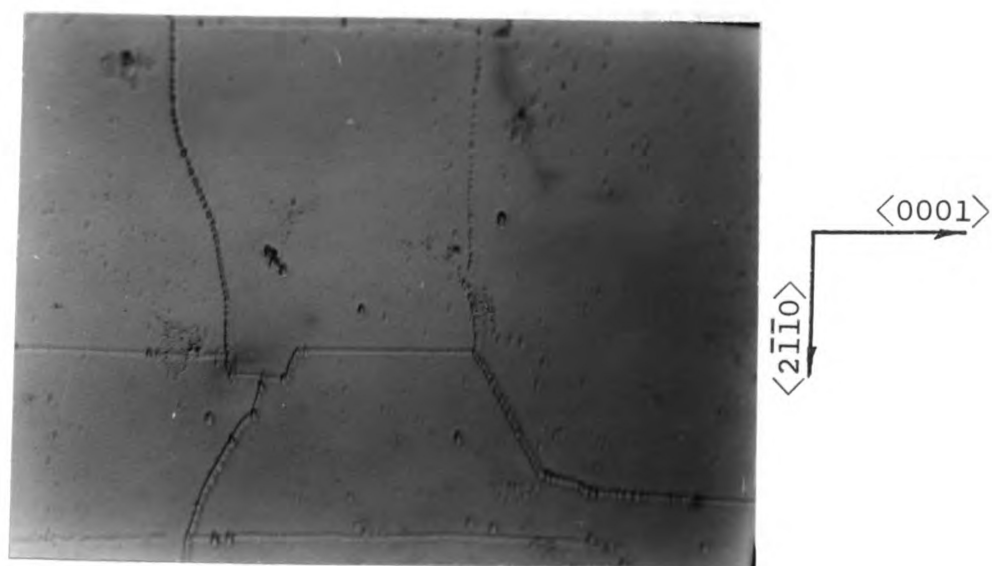
It is important to note that the offset method alone does not insure a crystal free from sub-boundaries in itself. In case of the crystal no. 2, the offset method alone did not improve the crystal perfection. However, in case

of crystals no. 31 and 33, all other improvements (such as the conduction sleeve, the insulation, the larger crucible, and the selection of good seed, etc.) are combined with the offset method to give the best results. In case of crystal no. 37, all the improvements without the offset method are not able to produce a sub-boundary free crystal. Crystal no. 37 reveals rather extensive sub-boundary distribution, despite the fact that the seed crystal was obtained from the crystal no. 33 which is one of the best crystals. The sub-boundaries present in crystal no. 37 might have originated from the welding of the seed to the polycrystalline specimen. This emphasizes again the importance of the offset method in eliminating the sub-boundaries.



$(10\bar{1}0)$

Fig. 8. Crystallographic arrangements of sub-boundaries.
500x



$(10\bar{1}0)$

Fig. 9. Crystallographic arrangements of sub-boundaries.
500x



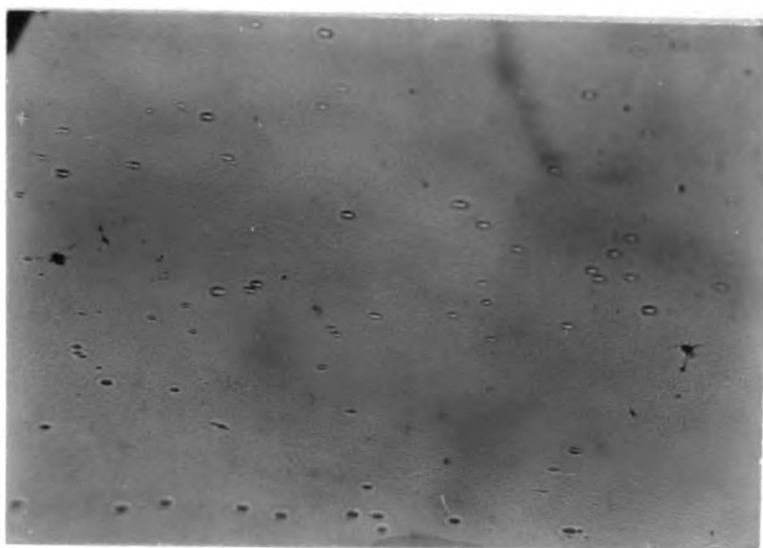
$(10\bar{1}0)$

Fig. 10. Sample with the orientation of 2-1.



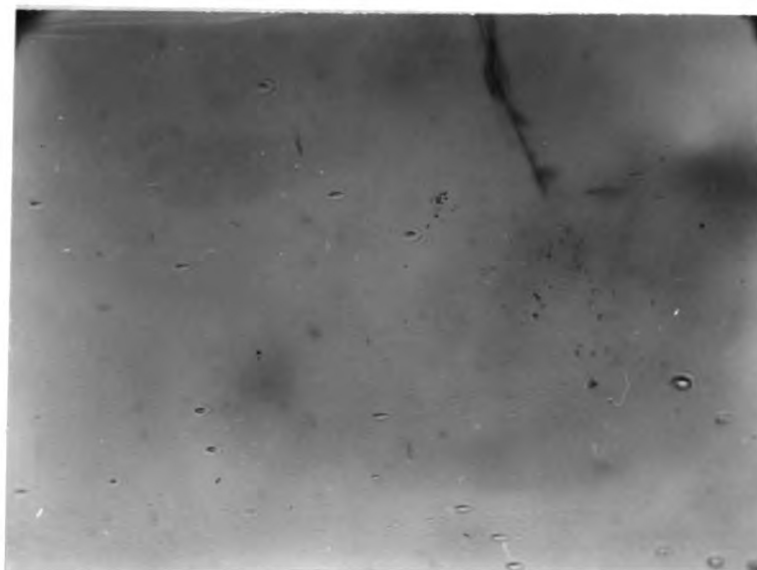
$(10\bar{1}0)$

Fig. 11. Sample with the orientation of 2-2. Sub-boundaries propagated from the seed. 320x



$(10\bar{1}0)$

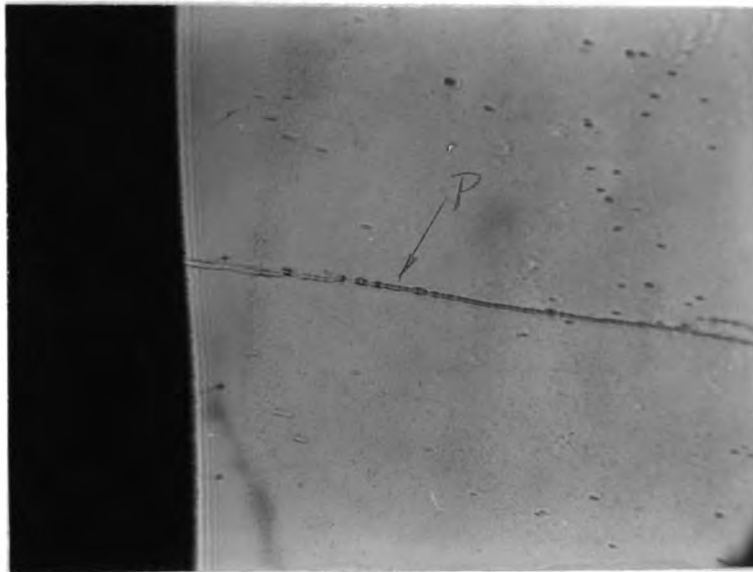
(a) Cross sectional surface.



$(10\bar{1}0)$

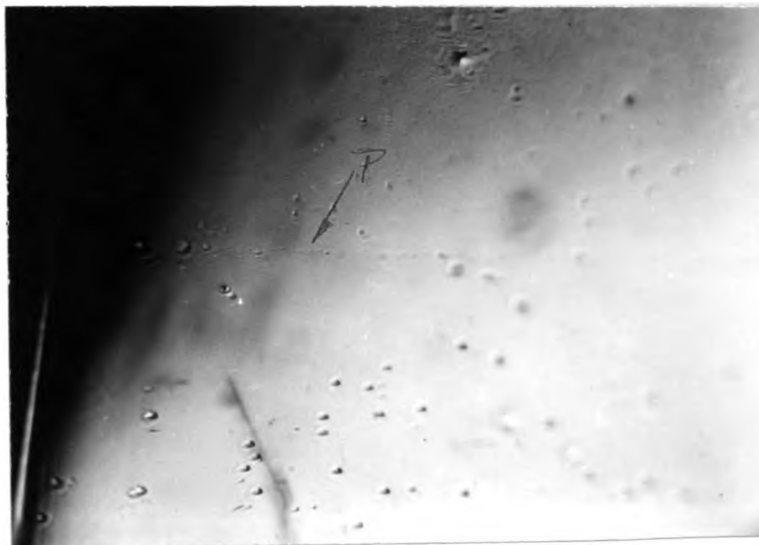
(b) Surface parallel to the growth direction.

Fig. 12. Background dislocations revealed on the cross sectional and the surface parallel to the growth direction of the crystal with the orientation 101. 500x. The crystal no. 31.



(10 $\bar{1}$ 0)

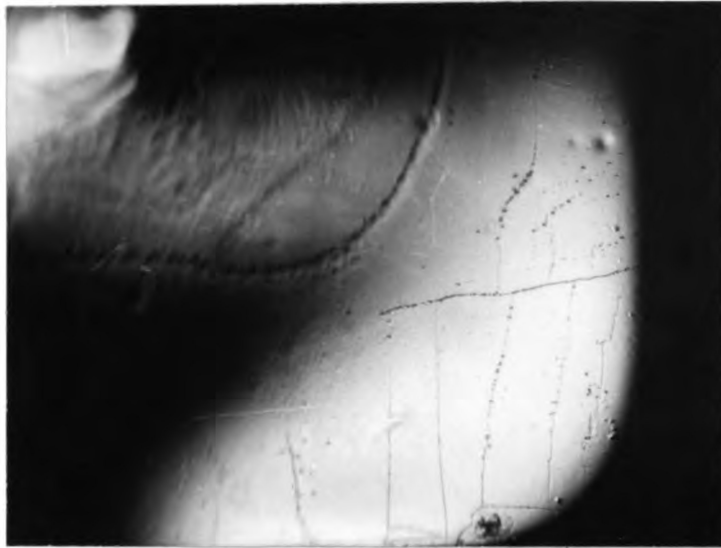
(a) Cross sectional surface.



(10 $\bar{1}$ 0)

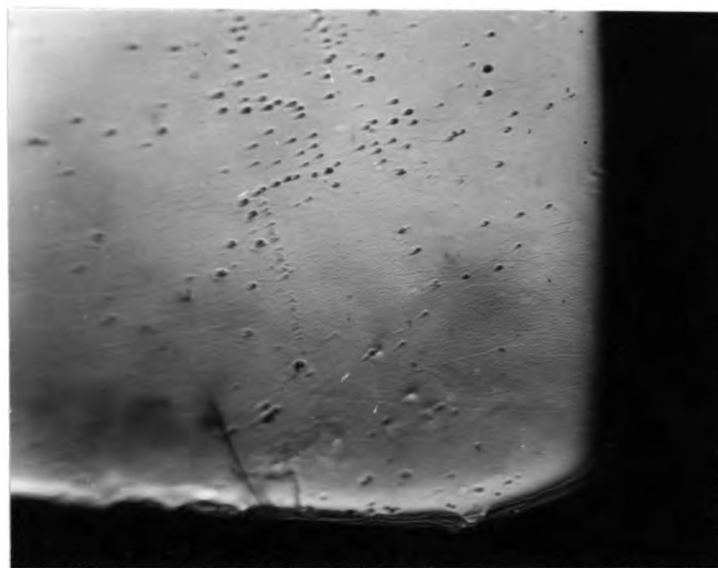
(b) Surface parallel to the growth direction.

Fig. 13. Sub-boundary etching on the cross sectional and the surface parallel to the growth direction of the crystal of the orientation 1-1. 500x. The crystal no. 31.



(10 $\bar{1}$ 0)

(a) Crystal grown in the crucible A



(10 $\bar{1}$ 0)

(b) Crystal grown in the crucible B

Fig. 14. Effect of crucible size on sub-boundary formation near a corner of the cross sectional surface. 500x

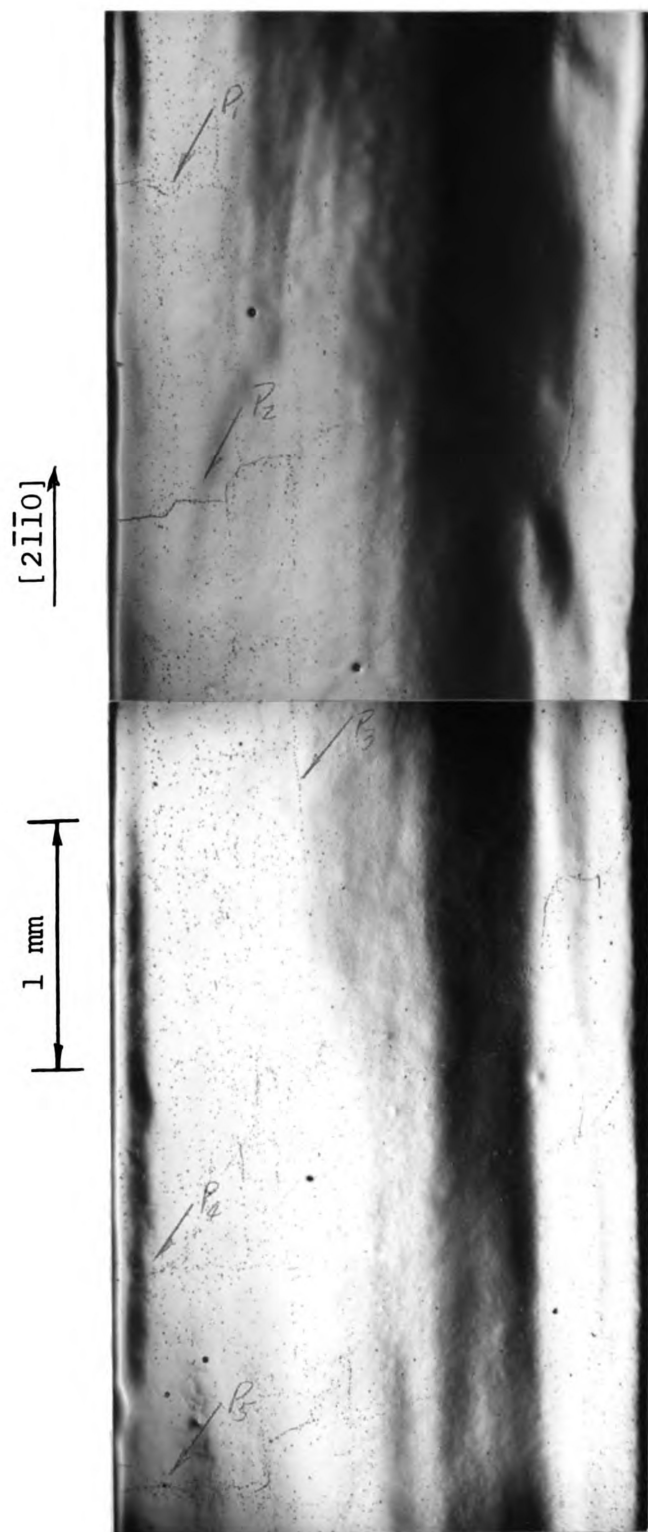
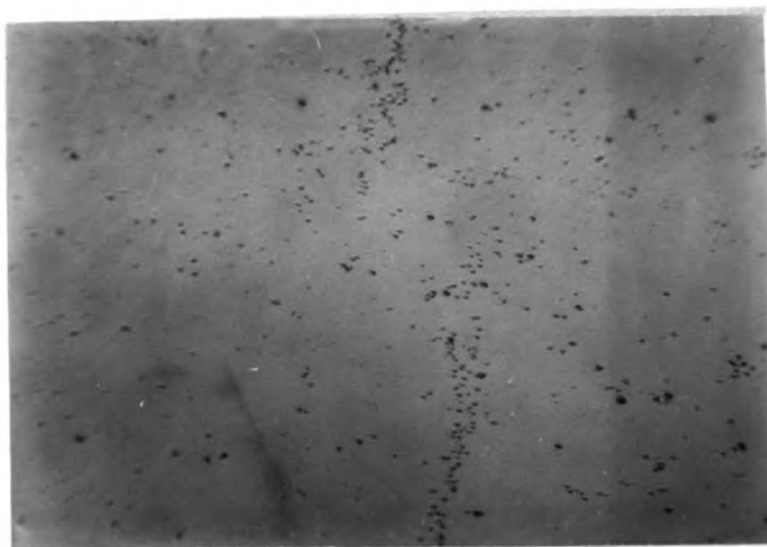
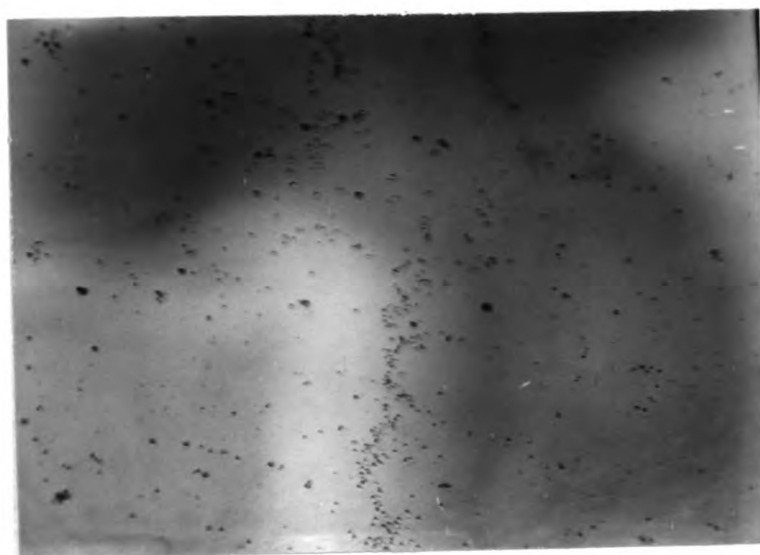


Fig. 15. Sub-boundaries on the (1010) cross sectional surface. 35x



(a)

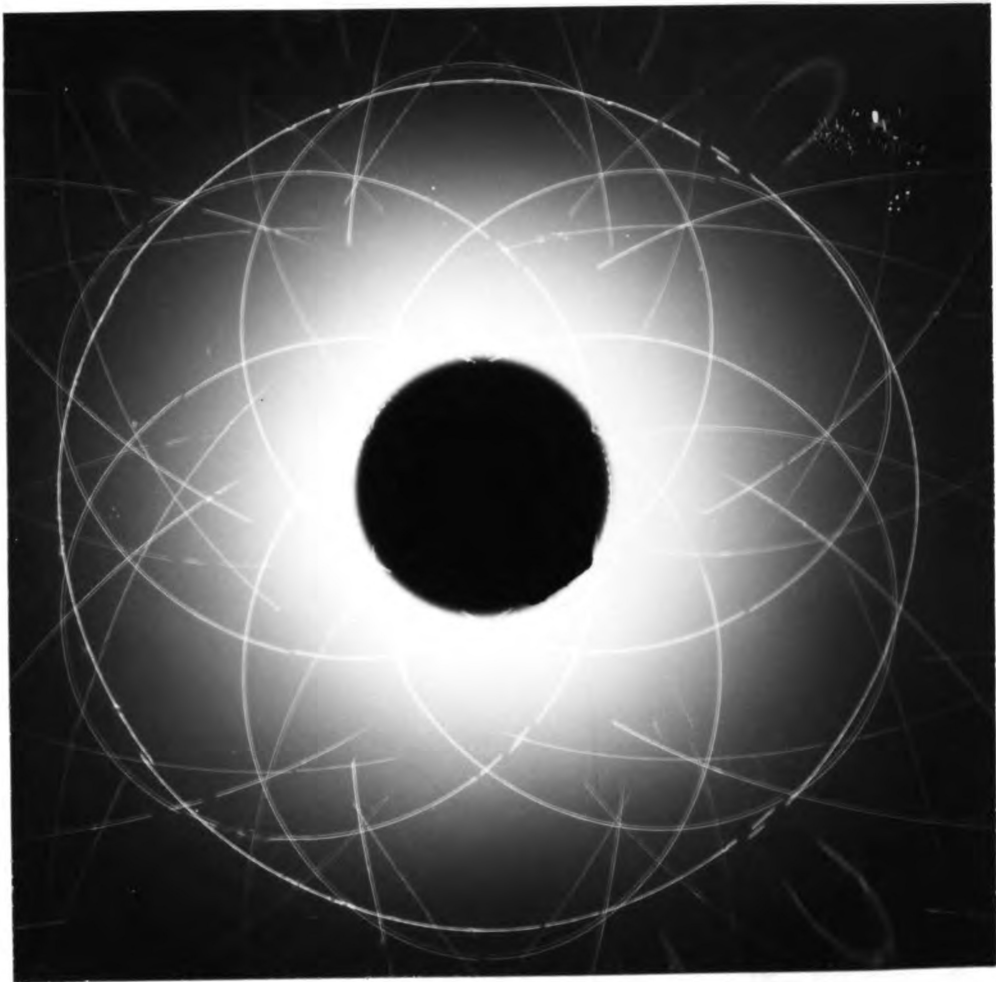


(b)

 $(10\bar{1}0)$

Fig. 16. Typical sub-boundaries formed at the faster cooling rate (2 mm/min.). 320x. The crystal no. 33.

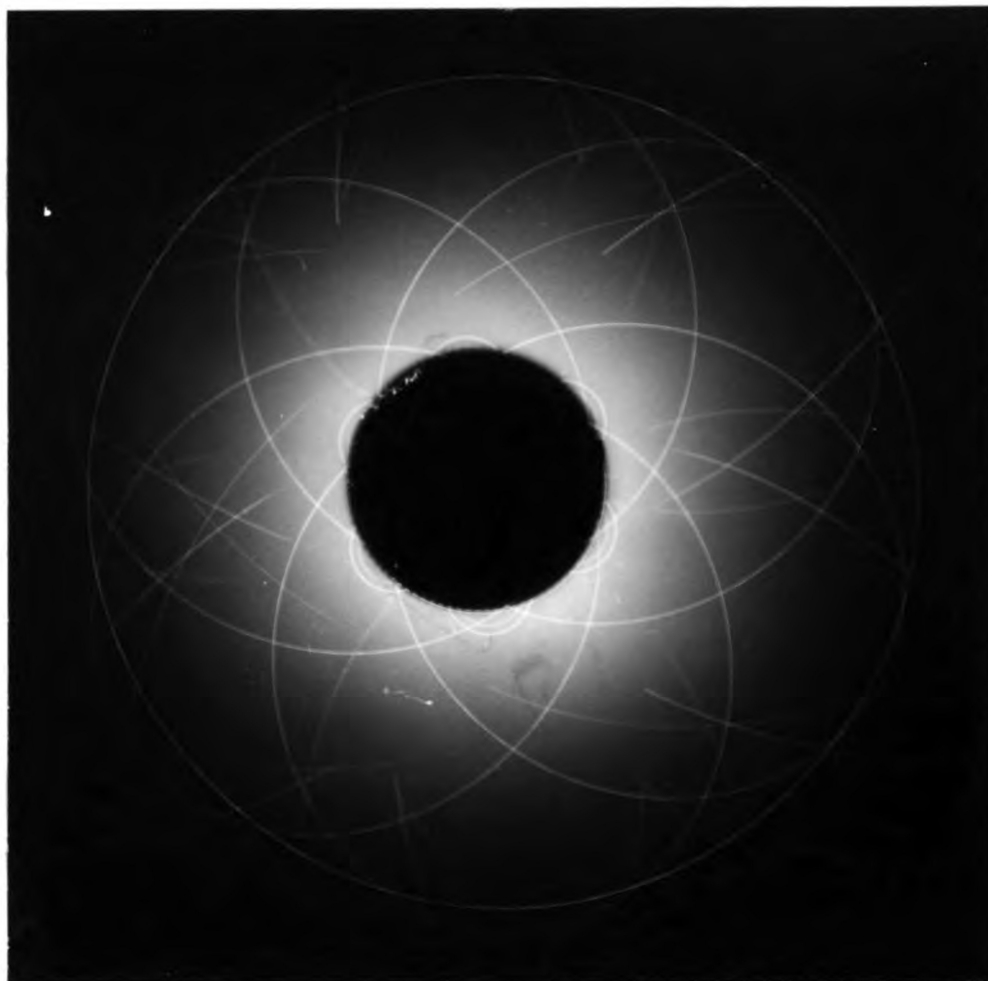
↑
Growth direction
 $\langle 10\bar{1}0 \rangle$



$(0001) \perp$ beam

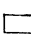
Fig. 17. Crystal Y. Microfocus x-ray back-reflection.

↑ Growth direction
 $\langle 10\bar{1}0 \rangle$



(0001) \perp beam

Fig. 18. Crystal C. Microfocus x-ray back-reflection.

Cryst. no.	Cryst. orient.	Seed orient.	Rate of growth mm/min.	Crucibles A or B	The cond. sleeve & insulation	Off-set method	Background dislocation density cm ²	Sub-boundary distribution	Remarks and origin of seed
1	1-1	1-1	0.55	A	no	no	1-5x10 ⁵	extensive	--
2	1-1	1-1	0.55	A	no	yes	"	"	--
19	2-1	2-1	1.0	"	yes	no	5-7x10 ⁴	"	--
20	2-2	2-1	1.0	"	"	"	"	"	--
32	2-1	2-1	"	B	"	"	"	"	--
30	1-3	1-1	"	A	"	yes	"	improved	--
32	2-3	2-1	"	A	"	no	"	somewhat	(a)  low sub-bdry high density
24	2-1	2-3	0.9	"	"	"	"	"	(b) portion of crystal no. 22
25	2-3	2-3	1.0	"	"	yes	"	"	(b) portion of crystal no. 22
31	1-1	1-3	1.0	B	"	"	6-9x10 ^{4*}	very low density	crystal no. 30
33	2-1	2-3	2.0	"	"	"	8-15x10 ^{4*}	"	(a) portion of crystal no. 22
36	2-1	2-3	1.0	"	"	"	5-7x10 ⁴	low density	(b) portion of crystal no. 22
34	2-1	2-1	0.55	"	"	"	"	moderate, many short sub-bdries	crystal no. 33
37	2-1	2-1	1.0	"	"	no	"	rather	"

* Total dislocation density + Cross section surface

TABLE I. Summary of the grown crystals

V. CONCLUSIONS

1. Highly perfect zinc single crystals of controlled orientations have been grown by improving the soft-mold technique.
 - a) The total dislocation density in the crystals is found to be about $6-9 \times 10^4 \text{ cm}^{-2}$.
 - b) The crystals are substantially free from sub-boundaries, except a few polygonized boundaries whose disorientations range from 5 to 30 sec. of arc, corresponding to $1-5 \times 10^3 \text{ cm}^{-1}$ in the linear density of dislocations. The average distance between the sub-boundaries is about 2 mm.
2. The sub-boundaries propagating from the seed can be eliminated by the offset method, under the condition in which no new sub-boundaries form during the growth.
3. The thermally induced stresses during the growth and the cooling to room temperature were substantially reduced by:
 - a) improving the axial heat conduction by the steel conduction sleeve;
 - b) preventing the radial heat loss by increasing the thermal insulation;

- c) providing a constant and uniform axial temperature gradient.
- 4. The polygonized sub-boundary increases in its disorientation as it traces from the interior to the free surface.
- 5. The etching technique is capable of measuring the disorientation of up to about 30 seconds of arc rather accurately at the magnification of 100x.
- 6. The dislocation lines and the sub-boundaries tend to run nearly parallel to the growth direction.
- 7. The pseudo Kossel patterns produced by the divergent X-ray method show a corresponding degree of crystal perfection to that of the etching technique.

VI. RECOMMENDATIONS

More refinements are needed in the crystal growth technique, and more data must be obtained for the growth of greater lattice perfection.

The present work does not prove that the thermally induced stresses are entirely responsible for the formation of dislocations and their arrays in zinc. It does not even prove that the thermally induced stresses are minimized. Thus, more attempts should be made to reduce the stresses even further:

1. Increasing the radial insulation by:
 - a) using the soft-mold material of lower thermal conductivity.
 - b) using larger crucible or smaller charge, thus increasing the thickness of thermal insulation.
2. Increasing the range of program cooling.

The zinc crystals grown in this work have been program cooled down to about 280°C . By extending the range of the program cooling to room temperature, the thermally induced stresses during the cooling would be reduced even further.

The effect of welding has not been well understood throughout this work. At no other occasion have the seed

crystals been subjected to such severe thermal stresses as during the welding. Such severe stresses are bound to have some effects on the distribution of dislocations in the seed crystal. In fact, this may well be the reason why the best crystals have not been obtained without employing the offset method. Thus, more recommendations are in order:

3. Development of a technique in which welding is not required for the controlled orientation of the seed, using the same growth technique.
4. Use of the Czochralski technique in which no welding is required.

In addition, there are some experiments which may be worthwhile for improvement of the crystal perfection.

5. Use of the seed crystals of the orientations 3-1 and 4-1 (refer to Fig. 4).

The dislocations lying in the basal plane would grow out of the crystal, resulting in a crystal free from the dislocations, provided that no new dislocations form during and after the growth. Here a question as to how the stresses, induced thermally or mechanically, would act on the weakness of the crystals accompanying the orientations 3-1 and 4-1.

6. Use of seed crystals in which most of the dislocation lines run nearly perpendicular to the specimen axis.

Such a seed can be obtained by cutting the pre-grown crystals horizontally.

Here again, a question concerning the effects of welding on the seed crystal arises. In this case, it would be advisable to employ the Czochralski technique.

REFERENCES

1. Darwin, C. F., Phil. Mag., v 43, p. 685 (1914).
2. Buerger, M. J., Z. Kristalloq. v 89, pp. 195 & 242 (1934).
3. Taylor, G. I., Proc. Roy. Soc., v A145, p. 362 (1934).
4. Orowan, E., Z. Phys., v 89, p. 634 (1934).
5. Dash, W. C., Growth and Perfection of Crystals, John Wiley and Sons, Inc., New York (1958), p. 361.
6. Bennett and Sawyer, "Single Crystals of Exceptional Perfection and Uniformity by Zone Leveling," Bell Sys. Tech. Journal, v 35, p. 637 (1956).
7. Elbaum, C., " D^{ns} in Metal Crystals Grown from the Melt," J. Appl. Phys., v 31, p. 1413 (1960).
8. Elbaum, C., "Dislocations Formed by the Collapse of Vacancy Discs," Phil. Mag., v 5, p. 669 (1960).
9. Howe and Elbaum, "Dislocation--Free Al Single Crystals," J. Appl. Phys., v 32, p. 742 (1961).
10. Brandt, Adams and Vreeland, Jr., "Etching of High Purity Zn," Calitech Res. Rept. (Dec. 1961).
11. Amelinck and Bontinck, "On the Generation of Dislocations in Melt-Grown Crystals," Acta Met., v 5, p. 345 (1957).
12. Chalmers, Bruce, "Effect of Impurities and Imperfections on Crystal Growth," Impurities and Imperfections, ASM v 84 (1954).
13. Chalmers, Bruce, J. Metals, New York, v 6, p. 519 (1954).
14. Frank, F. C., "Plastic Deformation of Crystalline Solids," Mellon Institute, p. 89 (1950).

15. Noggle, T. S., "A Soft Mold Tech. for Growing Single Crystals of Al," Rev. Sci. Instr., v 24, p. 184 (1953).
16. Teghtsoonian and Chalmers, "The Origin of Dislocations Grown from the Melt," Canad. J. Phys., v 29, p. 370 (1951); v 30, p. 388 (1952).
17. Verma, A. R., Crystal Growth and Dislocations, Butterworths Sci. Pub., London (1953).
18. Washburn, J., "Growth and Perfection of Crystals," John Wiley and Sons, Inc., New York (1958), p. 342.
19. Washburn and Nadeau, "On the Formation of Dislocation Substructures During Growth of a Crystal from Its Melts," Acta Met., v 6, p. 665 (1958).
20. Noggle and Koehler, "Crystal Perfection in Al Single Xtals," Acta Met., v 3, p. 260 (1955).
21. Kelly and Wei, "Lineage Str. in Al Single Crystal," Jnl. of Metals, v 7, p. 1041 (1955).
22. Guinier, Imperfections in Nearly Perfect Crystals, John Wiley and Sons, Inc., New York (1952), p. 402.
23. Lang, A. R., Jnl. Appl. Phys., v 29, p. 597 (1958); v 30, p. 1748 (1959).
24. Elbaum, C., "Substructures in Crystals Grown from the Melt," Progress in Metal Physics, v 203, p. 203, Pergamon Press Inc., New York (1959).
25. Lawson and Nielsen, Preparation of Single Crystals, Butterworths Sci. Pub., London (1958).
26. Seitz, F., Phys. Rev., v 79, p. 890 (1950).
27. Frank, F. C., Plastic Deformations in Crystalline Solids, Mellon Inst., p. 89 (1950).
28. Schoeck and Tiller, "On Disl. Formation by Vacancy Condensation," Phil. Mag., v 5, series 8, part 1, p. 43 (1960).

29. Frank, F. C. Deformation and Flow of Solids, IUTAM Colloquium Madrid (1955), p. 73.
30. Fuhlman and Wilsdorf, Phil. Mag., v 3, p. 125 (1958).
31. Aust and Chalmers, Canadian Jnl. Phys., v 36, p. 977 (1958).
32. Penning, P., "Generation of Imperfection in Ge Crystals by Thermal Strain," Philips Res. Rpts., v 13, p. 79 (1958).
33. Penning and Hornstra, "Birefringence Due to Residual Stress in Silicon," Phil. Res. Rpts., v 14, p. 237 (1959).
34. Buergers, J. M., Proc. Phy. Soc., London, v 42, p. 23 (1940).
35. Cottrell, A. H., Prog. Metal Phys. (1949), p. 77.
36. Billing, E., Proc. Roy. Soc., A235, p. 37 (1956).
37. Sinha and Beck, "Polygonization in Bent Zinc Crystals," Jnl. Appl. Phys., v 32, p. 1222 (1961).
38. Ball, C. J., "Surface Distributions of Dislocations in Metals," Phil. Mag., v 2 (20), p. 977 (1957).
39. Bell and Cahn, "The Dynamics of Twinning and the Interaction of Slips and Twinning in Zn Crystals," Proc. Roy. Soc., London, v 239, series A, p. 494 (195).
40. Bassi and Hugo, "Etch Pits in Zn," Jnl. Inst. Met., v 87, p. 376 (1958).
41. Dash, W. C., Jnl. Appl. Phys., v 29, p. 736 (1958); v 30, p. 459 (1959).
42. Gray, Hirsch and Kelly, "The Estimation of D Densities in Metals from X-ray Data," Acta Met., v 1, p. 315 (1953).
43. Gilman, J. J., "Etch Pits and Dislocations in Zn Monocrystals," Trans. AIME, v 206, p. 798 (1956).

44. George, Joy, "Dislocation Etch Pits in Zn Crystals," Phil. Mag., v 1, p. 803 (1956).
45. Gross and Werntroule, "The Growth from the Melt of Single Crystals of Low Melting Point Metals," Proc. Phys. Soc., v 65, Sec. B, p. 561 (1952).
46. Gross, A. J., "Heat Flow and the Growth of Metal Single Crystal from the Melt," Proceedings, Phys. Soc., London, v 66, Sec. B, Part 7, p. 525 (1953).
47. Rosenbaum, H. S., "Non-Basal Slip and Twin Accommodation in Zinc Crystals," Acta Met., v 9, p. 742 (1961).
48. Stepanova and Urusovskaya, "The Etch Method for Revealing Dislocations in Zn Crystals," Soviet Phys. Crystallography, v 4, p. 867 (1959).
49. Lambot, Vassamillet and Dejace, Acta Met., v 1, p. 711 (1953).
50. Schultz, L. G., Trans. AIME, v 200, p. 1082 (1954).
51. Fugiwara, T. and Takesita, I., "X-ray Reflection Patterns Produced by a Capillary X-ray Tube," J. of Science, Hiroshima University, Ser. A, v 2 (1941).
52. Imura, T., "A Study on the Deformation of Single Crystals by Divergent Beams"--Part I, Bulletin of Naniwa University, Ser. A, v 2, 51 (1954).
53. Imura, T., *ibid.*, Part II, Ser. A, v 5 (1957).
54. Lonsdale, K., Phil. Trans. Roy. Soc., London, Ser. A, v 240, 219 (1947).

ROOM USE ONLY

MICHIGAN STATE UNIVERSITY LIBRARIES



3 1293 03046 4154